Environmental Sciences Europe

RESEARCH

Open Access

Assessing the impact of the 2021 flood event on the archaeological heritage of the Rhineland (Germany)

Isabell Schmidt[1,2*], Bruno Boemke[3*], Irmela Herzog[1], Claudia Koppmann[1], Hannah Witte[1], Florian Sauer[4], Erich Claßen[1] and Frank Lehmkuhl[3]

Abstract

Background Archaeological sites are increasingly threatened by climate-related hazards. In response, heritage management authorities initiated projects to document damage and plan risk assessment measures. We present a project initiated after the heavy rainfall and subsequent flood event of July 2021, which involved extensive fieldwork to document the damage to archaeological sites in the Rhineland. We use this database to characterise and assess the damage and investigate site-specific and geospatial factors to identify potential predictive parameters for site damage.

Results During fieldwork, we found that the flood damaged 19% of the 538 archaeological sites surveyed. The majority of damaged sites are relatively recent, dating from the medieval or modern periods, and are associated with the use of water power. Damage was mainly caused by erosion, floating debris and washout, e.g. mortar. In a case study, we tested the option of comparing pre- and post-disaster Airborne Laser Scanning elevation data to identify damages. It showed that not only the damage detected during fieldwork was found but also additional areas of loss. In general, however, and quantified based on the entire dataset, the ordnance survey Airborne Laser Scanning data were of limited use for monitoring flood-related damage and could not replace fieldwork. Our statistical analysis of possible risk factors, including both site characteristics and geospatial parameters, using Naïve Bayes Modelling and chi-squared tests, showed that no set of parameters could consistently predict the preservation or damage of archaeological sites across all catchments. In contrast, some external geospatial factors correlated with the occurrence of damage.

Conclusions The study highlights both the strengths and limitations of the approaches used to assess and predict the damage to the archaeological heritage in the 2021 flood zones of the Rhineland. It also demonstrates the complexity of the data and spatial processes involved, which limits generalisation but can still inform decision-making for archaeological site management and on-site protection measures in flood-prone areas. With the prospect of more frequent heavy rainfall due to climate change, the specific needs of the archaeological heritage should be integrated into broader prevention and disaster management plans.

Keywords Archaeological site, Natural hazards, Damage assessment, Prevention measures, Disaster protection plans, Airborne laser scanning

*Correspondence:
Isabell Schmidt
isabell.schmidt@uni-koeln.de
Bruno Boemke
bruno.boemke@geo.rwth-aachen.de
Full list of author information is available at the end of the article

Springer Open

© The Author(s) 2024. **Open Access** This article is licensed under a Creative Commons Attribution 4.0 International License, which permits use, sharing, adaptation, distribution and reproduction in any medium or format, as long as you give appropriate credit to the original author(s) and the source, provide a link to the Creative Commons licence, and indicate if changes were made. The images or other third party material in this article are included in the article's Creative Commons licence, unless indicated otherwise in a credit line to the material. If material is not included in the article's Creative Commons licence and your intended use is not permitted by statutory regulation or exceeds the permitted use, you will need to obtain permission directly from the copyright holder. To view a copy of this licence, visit http://creativecommons.org/licenses/by/4.0/.

Background

The exceptionally heavy rainfall and the subsequent flooding of areas of western Germany, Belgium and the Netherlands in the summer of 2021 caused devastating damage to people, buildings, infrastructure, and nature [1–3]. As a result of climate change, such extreme weather events are expected to become more frequent in the future [4–8]. This has led to an intensive discourse on how to deal with cultural heritage sites threatened by climate change and how to assess the vulnerability of sites, their risk of damage, and their resilience [8–12]. In line with these efforts, data on damage caused by hydrometeorological disasters are a valuable source to inform many aspects of this discussion (e.g., [11, 13]). However, such data are not widely available for archaeological sites and registered archaeological monuments. Moreover, studies often focus on prominent world heritage sites or other officially registered monuments. The archaeological record affected by hydrometeorological hazards at the level of municipalities and regional councils includes many different sites with a wide variety of specific properties and characteristics, spatial dimensions, materials and local settings. A better understanding of the diverse set of factors that cause damage to a site is needed to inform protection, conservation and mitigation measures.

Although concerns about the preservation of archaeological sites may seem marginal compared to the loss of human life, homes and the damage to critical infrastructure, there are generally accepted reasons, such as the impact of cultural heritage on social cohesion and sustainable development [14], and a statutory obligation to preserve, maintain and protect archaeological sites, which is laid down for our study area by the North Rhine-Westphalia (NRW) Monument Protection Act [15]. In order to record and quantify the damage to archaeological sites caused by the flood event in NRW in July 2021, two projects were initiated, focusing on the most affected areas [16]. While the results of the project carried out by the Regional Association of Westphalia-Lippe (Archäologie für Westfalen, Olpe, LWL-AfW) are presented elsewhere [17], the data reported here originate from the project 'Flood Damage Register 2021' [18–20], carried out by the LVR-State Service for Archaeological Heritage in the Rhineland (LVR-ABR). Archaeological sites were inspected, and damage was documented through descriptions, photographs, and mapping. The findings were reported to 22 municipalities which were selected based on a heuristic assessment of an expected high amount of damage. Reports included a scientific damage assessment, mitigation recommendations, and, where applicable, preventive protection measures [20].

The extensive fieldwork conducted during the project to assess the damage had raised the question to what extent available remote sensing techniques could reduce or replace the work on-site. To this end, we evaluated the database on damaged archaeological sites and compared also ordnance survey Airborne Laser Scanning (ALS) elevation data recorded before and after the flood event. To understand the factors involved in creating the damage, we analysed the spatial, qualitative and quantitative data obtained during the project. A distinction between internal and external factors was made, where internal factors comprise qualitative and quantitative data on the type, age and material of each archaeological site, and external factors include geospatial data on hydrology, topography, soil and land use. This distinction between internal and external factors differs partly from previously proposed risk and vulnerability assessment systems in heritage management (e.g. [11, 14]). The factors are therefore made explicit in the following analysis to allow for future reorganisation.

The rainfall and flood event from July 2021 in the study area

Our investigations focused on areas in the Lower Rhine Embayment and adjacent low mountain ranges (Fig. 1:a), a region defined by the responsibilities of the LVR-ABR. The rainfall and the subsequent flood from July 2021 [2, 5, 21] particularly affected two areas: firstly large parts of the low mountain ranges in the south-western area, that is the Eifel and the transition regions to the embayment, e.g. the Jülich-Zülpicher Börde. It comprises the catchment areas of the Rur and Erft rivers, but also parts of the Kyll and Aar (Fig. 1:b). Secondly, in the eastern part, i.e. on the right side of the Rhine River, the low mountain ranges of the Bergisches Land also received a lot of rainfall (Fig. 1:c), affecting the catchment areas of the Wupper and Sieg rivers as well as transitional areas to the Rhine catchment. The geomorphological impact of pluvial floods in the Central European uplands differs from that of floods in transitional areas and the lowland rivers due to their flash flood characteristics (Table 1). Narrow and often steep valleys, combined with thin and saturated soils and thus reduced retention potential, promote rapid surface runoff on slopes and, hence, a rapidly rising flood hydrograph. This is further aggravated by the mostly narrow river valleys [5, 21]. The floods caused less damage in the lowlands because the flow velocities are lower and there are fewer obstacles, such as boulders, trees, cars, and other debris. Particularly noteworthy are, however, the catastrophic breakthroughs of the river Inde near Inden into the open-cast mine of the same name and the Erft into a gravel pit near Erftstadt-Blessem [22]. These events caused enormous erosion but at the same

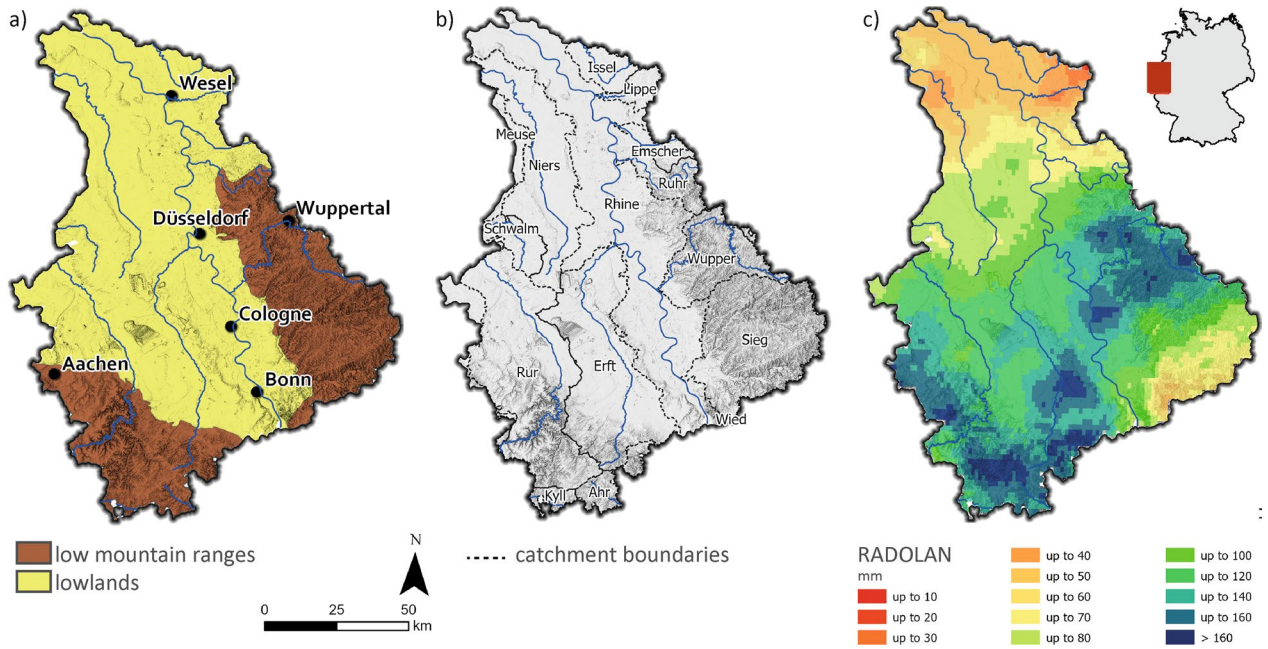


Fig. 1 Map **a** showing the basic landscape forms of the working area of the LVR-ABR: the low mountain ranges and lowlands. The main river systems are indicated in blue, and dashed lines in **b** describe the watersheds of the main drainage basins. The precipitation during the rainfall event from 12th to 15th of July 2021 (**c**, after [24] hourly RADOLAN-raster of precipitation (binary), Version 2,5)

Table 1 *Summary of the geomorphological impacts of the flash flood and flooding of the 2021 flood event in the low mountain ranges of the Eifel and the lowlands of the Lower Rhine Embayment. Modified according to* [25]

Low mountain ranges	Lowlands
Flash floods	*Flooding*
Steep and short flood wave	Shallow and long flood wave
High flow velocities	Reduced flow velocities
Short reaction time	Longer reaction time
Available material: rubble, rock	Available material: fine fractions, sand
Accumulation mainly of gravel	Accumulation mainly of fine-grained sediments
High damage potential on buildings and infrastructure	Flooding of areas—but less damage potential

time stored water, resulting in less flooding downstream. With increasing distance from the low mountain ranges, the orographic gradients are decreasing, so very high water levels were recorded in the lowlands with decreasing energy and flow speed [2]. In contrast to other floods, the wide Rhine plain absorbed and diverted a large part of the outflowing water masses [22, 23].

Material and Methods

The database of archaeological sites at risk of flooding

Our database comprises 538 archaeological sites located in areas exposed to flood events. For the data compilation, georeferenced data and background information on the archaeological sites were readily available from the LVR-ABR-internal information system with a GIS component, so-called BODEON [26]. In a first working step, all known archaeological sites were considered, regardless whether they have a protection status as registered archaeological monuments, are presumed monuments or recorded as so-called archaeological 'activities'. By statutory definition of the State of NRW [15] archaeological sites are or were at some point in time in the ground or under water. This way they should not be confused with architectural monuments, although they may also include construction elements and buildings (masonry/foundation areas, dams, sluices gates, etc.) or are located below or next to architectural monuments.

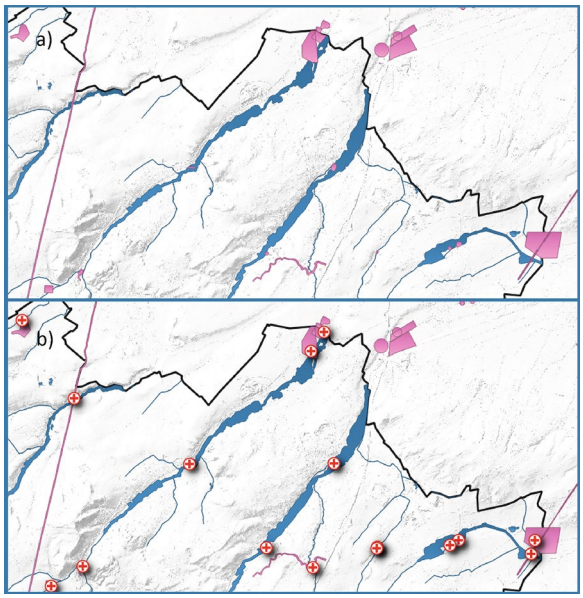


Fig. 2 Exemplary map-section to illustrate **a** the query result on archaeological site data from the LVR-ABR internal application BODEON (pink areas) and the compiled hydrological data (20 m buffered flood risk mapping, 3 m buffered river data, real flood mapping). Map **b** shows the evaluated points of interest (POI), which were later inspected during fieldwork

In a second working step, and in order to focus on sites located in flood-affected areas, we used publicly available flood-hazard maps [22]. As the flood in 2021 even exceeded the level of the available most extreme scenario ('HQextrem') in some places, the extreme scenario areas were extended by a buffer of 20 m. We also added water station maps for smaller rivers, streams and rivulets [27], which we buffered by 3 m. This compilation of hydrological information (Fig. 2:a) proved to be entirely adequate when compared to observed local maximum water levels (e.g. [28]) or actual flood maps derived from satellite data [29, 30]. Due to the semi-automatic classification of water surfaces, the latter were frequently distorted by areas with very shallow water depths and no acute hazard potential for archaeological sites.

The third step comprised the creation of 'Points of Interest' (POI) at intersections of archaeological data from BODEON with the hydrological data (Fig. 2:b). In order to reduce workload in the field, the sites were then again evaluated, removing, e.g. sites that no longer exist (removed or rebuilt) or are located under intact built-up areas. All remaining archaeological sites were visited and inspected in the field.

When damage was detected during fieldwork, quantitative and qualitative data were recorded according to the LVR-ABR internal recording system. This also applied to previously unknown archaeological sites that were discovered during fieldwork. In addition, information on the spatial extent of the damage was recorded in the field to create polygons representing only the damaged parts of each site for later use in geostatistical analysis. In some cases, especially urban/village areas, renovation work on archaeological sites or building complexes located on them had already been completed at the time of our assessment, some archaeological sites were inaccessible. In these cases, they could not be included.

During the final processing of data from damaged sites, additional information was recorded: the current use of the site's area, its general condition, the material that was damaged by the flood, and a characterisation of the intensity of the damage. For the latter, the guiding question of the project was: 'Is conservation mitigation required or not?' (Minor = no mitigation required, Medium = mitigation recommended, Major = mitigation required / lost). In order to facilitate a functional workflow, a set of simplified, coarser categories was laid out for the type of site, its chronological position, and the type of damage observed. For the statistical analysis, only the most prominent period and type of damage were considered for each archaeological site, although often different periods and types of damage were present.

Geostatistical analysis

The geostatistical analysis aims to determine whether the internal or external factors can explain the occurrence of damage. To this end, a set of physiographic parameters with a possible influence on the local damage potential of the flood was compiled. An overview of all selected parameters, their possible influence on the damage potential, and their source is given in Table 2. For a first impression and a coarse overview of their spatial behaviour, four of the parameters are additionally visualised in Fig. 3. In preparation for the statistical analysis, the values of all physiographic parameters were extracted at the location of the archaeological sites or, if damage were observed in the field, for the damaged area. This extraction was conducted using the GIS software ArcGIS Pro 3.3. As the sites in the compiled database are stored as polygons, spatial aggregations had to be performed to extract only one physiographic value per site. For parameters in raster format, zonal statistics were calculated by extracting either the majority (aspect, TPI, DEV), mean (slope, cost distance, REM) or maximum (flow- and precipitation accumulation) value within the site polygon (ArcGIS Pro Tool: Zonal statistics as table). For parameters in vector format, spatial joins were conducted, adding the information of the parameter with the largest overlap or closest to the site polygon (ArcGIS Pro Tool: Spatial join). This extraction process results in a tabular

database containing all archaeological sites, each with an aggregated physiographic value attributed to them.

This tabular database was then used as input for a statistical analysis using the IBM SPSS statistics software. In this analysis, the site damage assessment was treated as the dependent variable, while internal (site type and chronology) and external (physiographic) site parameters were treated as independent variables. Discriminant analysis [32, 33] and Naïve Bayes [34, 35] probability analysis were applied to test whether or not the damage assessment could be explained by external factors. Both methods use the values of all independent variables to build a predictive model based on a known group membership (in this case damaged/undamaged). The comparison between actual and predicted group membership then allows an assessment of the strength of the combined parameters in predicting the occurrence of damage. In addition, the Naive Bayes method assesses the individual relative importance of the independent variables in predicting damage occurrence, allowing them to be ranked in terms of their predictive strength. In both predictive analyses, the tabular site database was evaluated both as a whole and by river catchments. Naïve Bayes was chosen as the main statistical method for this approach as it allows a comparison of categorical and continuous variables and is highly resistant towards irrelevant parameters.

In addition to this multi-factor approach, the statistical associations between the occurrence of damage and individual external factors from the tabular database were tested by applying the chi-squared (χ^2) hypothesis approach (using the statistical software package Past, v3.2). A χ^2 test is used to assess indications of statistical independence of the distribution of two categorial datasets. The external factors were first categorised for these tests, focusing on similar class sizes. The two states *damaged* and *undamaged* were then compared to test for dependencies on external factors, which do not necessarily indicate causation.

Remote sensing using ALS elevation data

The approach used in our study to remotely assess the extent of damage is to analyse the difference between the terrain surfaces derived from ALS elevation data from before and after a defined moment in time [36]. The methodology relies on open access ALS data preprocessed by the ordnance survey institution Geobasis NRW because this data is readily available. In this way, the potential and limitations of using ALS data to detect damage to archaeological sites can be investigated with limited effort. Possible refinements of this approach involving additional effort are outlined in the 'Discussion' section. Geobasis NRW schedules ALS flights in winter, i.e. in off-leave conditions. Classified ALS elevation points are provided, with an elevation accuracy of 15 cm (two standard deviations). In general, between 4 and 8 ground points are typically available per square metre. The first step of our methodology is the linear TIN (Triangulated Irregular Network) interpolation of the two ground point datasets to be compared [37]. This interpolation method ensures that the elevation values of the ground points are exactly reproduced by the resulting surface and that the elevation estimate for each point is in the range of its nearest ground point neighbours. Where photographs of the archaeological site show building remains, manually selected non-ground ALS points are added to the point cloud prior to the interpolation. Unfortunately, the ALS point classification by Geobasis NRW assigns elevation points on wall remains to the 'Last Return not ground' class, in which points on trees or cars can also be found. This complicates the identification of elevation points on the remains of walls. The two resulting raster DTMs with a cell size of 0.2 m are checked to see if one of the DTMs needs to be shifted before subtraction. This is performed by comparison of artificial cross sections located in unchanged parts of the study area [38]. In previous studies, shifts in x, y, and z-direction turned out to be necessary. But in the two cases described below, no shift was required. Obviously, the number of ground points per square metre determines the minimum size of objects that this methodology can detect. According to the Nyquist limit, to identify a circular pit with a diameter of 1 m in a DEM, the maximum distance within the set of altitude points forming the basis of the DEM should not exceed 0.5 m, and 0.25 m is the recommended maximum distance [39]. Therefore, the average ALS ground point density is not the only limiting factor; gaps in the ALS data may obscure the presence of damage or identify false positives. To account for these gaps in the ALS data, a 1 m grid is created for both DEMs, storing the number of ground points within each cell. After this pre-processing, the difference map is created by subtraction. Contour lines are generated at 0.15 m intervals for the resulting grid, i.e. the accuracy of the ALS points. For the example presented below, areas of possible loss are delimited by the 0.45 m contour line. If any of these areas overlap with an area without ground points in any of the two DEMs, the overlapping area is subtracted. The resulting set of areas of possible loss is reduced by deleting all areas which cover less than 1 square metre. It is checked for areas of less than 4 square metres, if the difference is based on several ground points. Aerial photographs provided by Geobasis NRW or other institutions are sometimes useful to explain the cause of differences. However, most of the watercourses in the Rhineland are bordered by bushes or trees, which block the view on sites close to the water.

Table 2 Overview of the external factors used in the geospatial analysis, including the name of the factor, a brief explanation of the possible influences on the flood damage potential, the data type and the source

Parameter	*Explanation*	*Type*	*Source*
DLM	Digital land use model. Contains detailed information on land use classes such as forest, agriculture and urban areas. Used in this study as an indicator of erodibility and anthropogenic impact	Vector dataset with polygons	https://www.opengeodata.nrw.de/produkte/geobasis/lm/akt/basis-dlm/
BK50	Digital soil map. Contains information on soil depth, type, substrate and erodibility. All four parameters were included in the statistical analysis	Vector dataset with polygons	https://open.nrw/dataset/ab0f265c-dabe-4bcd-869a-d97dc328c141
GSK3E	Assessment of the naturalness of a riverbed and the surrounding floodplain. An important parameter for hydraulic processes such as channelling effects. Only available for a small subset of rivers in the area of interest	Vector dataset with lines	https://www.lanuv.nrw.de/umwelt/wasser/oberflaechengewaesserfluesse-und-seen/fliessgewaesser/gewaesser-stationierungskarte/
Slope	Topographic parameter that heavily influences local flow speed and thereby the destructibility of flood water	Raster dataset with 1*1 m resolution	Derived dataset based on https://www.opengeodata.nrw.de/produkte/geobasis/hm/dgm1_xyz/
Aspect	Topographic parameter that influences the solar input and thereby slope stability as well as potential vegetation cover. This parameter was reclassified into the 8 cardinal directions	Raster dataset with 1*1 m resolution	Derived dataset based on https://www.opengeodata.nrw.de/produkte/geobasis/hm/dgm1_xyz/
TPI	Topographic position index, describing the elevation of a point in comparison to the mean elevation of the surroundings (reclassified into ridge, upper slop, middle slop/flat, lower slope, valley). Used in this study to compare the location of sites within their respective riverbed	Raster dataset with 1*1 m resolution	Derived dataset based on https://www.opengeodata.nrw.de/produkte/geobasis/hm/dgm1_xyz/
DEV	Deviation from mean elevation. Topographic parameter similar to the TPI but additionally scaled by the local ruggedness (standard deviation of elevation) for the comparison of heterogeneous landscapes. See [31] for more information on TPI and DEV	Raster dataset with 1*1 m resolution	Derived dataset based on https://www.opengeodata.nrw.de/produkte/geobasis/hm/dgm1_xyz/
Rivers	Hydrological network derived from a digital elevation model via filling, flow direction and flow accumulation tools. Used to calculate the distance from the nearest river as well as the mean or max slope of the nearest river segment	Vector dataset with lines	Derived dataset based on https://www.opengeodata.nrw.de/produkte/geobasis/hm/dgm1_xyz/
REM	Relative elevation model, displaying the height above the nearest river. An important parameter for assessing the areas that can be reached by the flood	Raster dataset with 1*1 m resolution	Derived dataset based on https://www.opengeodata.nrw.de/produkte/geobasis/hm/dgm1_xyz/
Cost distance	Distance of a site to the nearest river, but weighted by the slope that occurs within the traversed surface. Similar to the REM, it allows an assessment of probability that the flooding reached the site	Raster dataset with 1*1 m resolution	Derived dataset based on https://www.opengeodata.nrw.de/produkte/geobasis/hm/dgm1_xyz/
Flow accumulation	The number of DEM cells that drain into the site polygon according to slope and aspect. Allows an assessment of the potential water masses that reach the site in case of a precipitation event	Raster dataset with 1*1 m resolution	Derived dataset based on https://www.opengeodata.nrw.de/produkte/geobasis/hm/dgm1_xyz/

Table 2 (continued)

Parameter	*Explanation*	*Type*	*Source*
River flow accumulation	The number of DEM cells that drain into the largest river within a 100 m distance of the site polygon. Allows an assessment of the potential magnitude of discharge in the closest river in case of a precipitation event	Raster dataset with 1*1 m resolution	Derived dataset based on https://www.opengeodata.nrw.de/produkte/geobasis/hm/dgm1_xyz/
Precipitation accumulation	The flow accumulation multiplied by the precipitation that was recorded during the July 2021 flood event. Represents the water masses that crossed the sites during the event when only considering surface discharge	Raster dataset with 1*1 m resolution	Derived dataset based on https://www.opengeodata.nrw.de/produkte/geobasis/hm/dgm1_xyz/ and https://opendata.dwd.de/climate_environment/CDC/grids_germany/daily/radolan/
River precipitation accumulation	The river flow accumulation multiplied by the precipitation that was recorded during the July 2021 flood event. Represents the discharge in the closest river during the event when only considering surface discharge	Raster dataset with 1*1 m resolution	Derived dataset based on https://www.opengeodata.nrw.de/produkte/geobasis/hm/dgm1_xyz/ and https://opendata.dwd.de/climate_environment/CDC/grids_germany/daily/radolan/

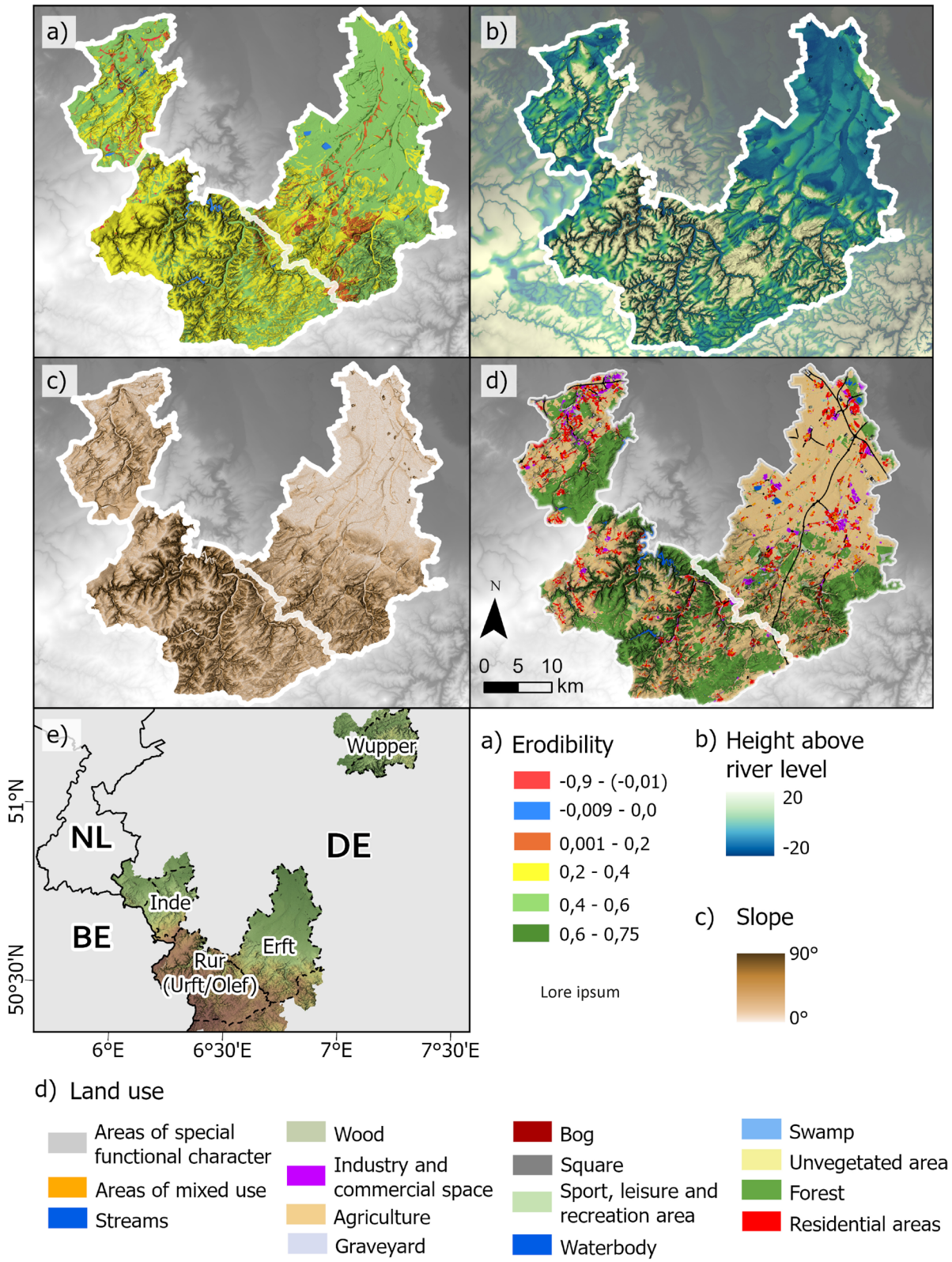


Fig. 3 Spatial examples for four selected external parameters, including **a** soil erodibility, **b** height above river level (REM), **c** slope and **d** current land use (DLM). The investigated areas are coloured in **e**, with dotted lines delimiting the studied partial river catchments referred to in Table 4. Note that the Wupper catchment area is not shown to improve map readability

To evaluate the applicability, potential and limitation of this ALS-based approach in the context of a catastrophic flood event, we first tested it on two sites recorded during the project. Secondly, we used the project's database to assess which of our recorded damage would have potentially been identifiable by the chosen remote sensing approach [40].

Results

Out of a total of 538 analysed sites, damage was documented at 103 sites (19%, see Fig. 4). This includes 18 previously unknown sites that show flood induced damage and have been recorded for the first time. In the following sections, the data will be analysed by first looking at internal factors, followed by internal and external factors and finally, the applicability of ALS data for the detection of the damage.

Internal factors for damage to archaeological sites

Chronology

Although the chronological position of all the potentially affected sites shows an already clearly skewed distribution towards sites of more recent periods (i.e. the Middle Ages and especially the Modern Era, Fig. 5:a), the flood damage occurred mainly at sites of the more recent periods. This is also true of the relative frequencies within each period (Fig. 5:b): 13% of the Roman sites, 17% of Medieval sites and 24% of Modern sites are affected. Pre-Roman archaeological sites (Stone Age or Metal Age sites) are practically absent in the valleys studied.

Site types

The most frequently damaged site type in the investigated regions are clearly water powered grinding mills or hammering systems. They dominate the total number of archaeological sites investigated (n = 208) and make up half of the damaged sites (Table 3, see also the statistical results presented Table 5). Weirs, sluice gates, and dams were most frequently damaged, as were ditches and their lateral stabilisations. The percentage of damage to archaeological remains related to castles, monasteries and quadrangles is lower than for water powered systems, but 12% of the total damage was associated to the moats, buildings' fundaments or enclosing walls. The next most frequently damaged category is 'water management' relicts, which includes all systems that served the water supply in general, beyond mills or hammer mills, but mainly including sites from the Roman Period, i.e. the Eifel aqueduct.

The remaining types of damaged archaeological sites are quite diverse. Table 3 lists paths, fords, bridges, fall shafts and adits, charcoal kilns and smelting sites, relics of the Second World War, as well as industrial facilities. No flood damage was observed on ditches and earth banks, burial grounds or in quarries.

Specific causes of damage

The most common types of damage occurred repeatedly at similar archaeological site types. Erosion of soil material was the most prominent cause of damage (57%). It was observed along the banks of streams or ditches, especially on steep slopes, but also often in the immediate vicinity of the remains of walls and buildings. In the latter case, turbulences also led to deep scouring, exposing foundations and even causing cracks in the rising masonry. A small but regular proportion of erosion damage (8%) was caused by breaches in embankments. They occurred mainly in medieval to modern mill and hammer ponds. Erosion damage was rarely observed in open areas, on cultivated arable land or pastureland.

Another cause of damage, floating debris such as branches and building materials, caused damage mainly to structural elements in streams and ditches, such as the crowns of weirs or sluices (15%). Damage to masonry (12%) was often associated with the washing out of joint sealants. This occurred particularly in the case of remains of Roman structures located above ground, i.e. again the Eifel aqueduct. To a lesser extent, damage was also

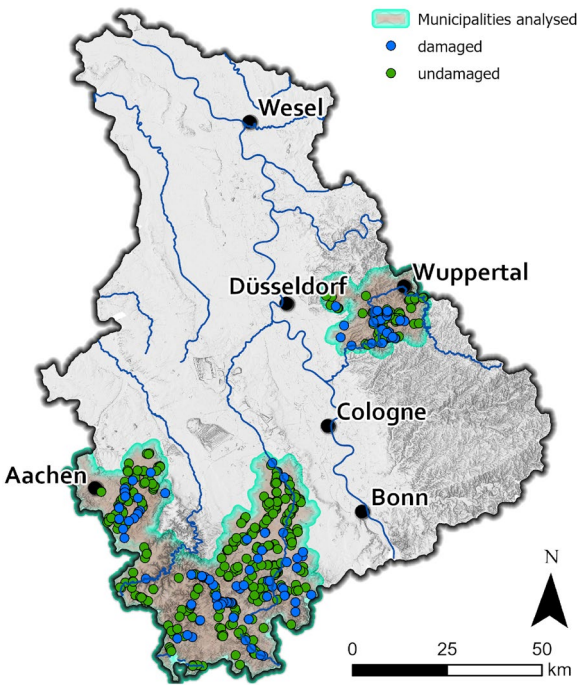


Fig. 4 The distribution of archaeological sites considered in this study (damaged = blue, undamaged = green). The surveyed municipalities are shaded

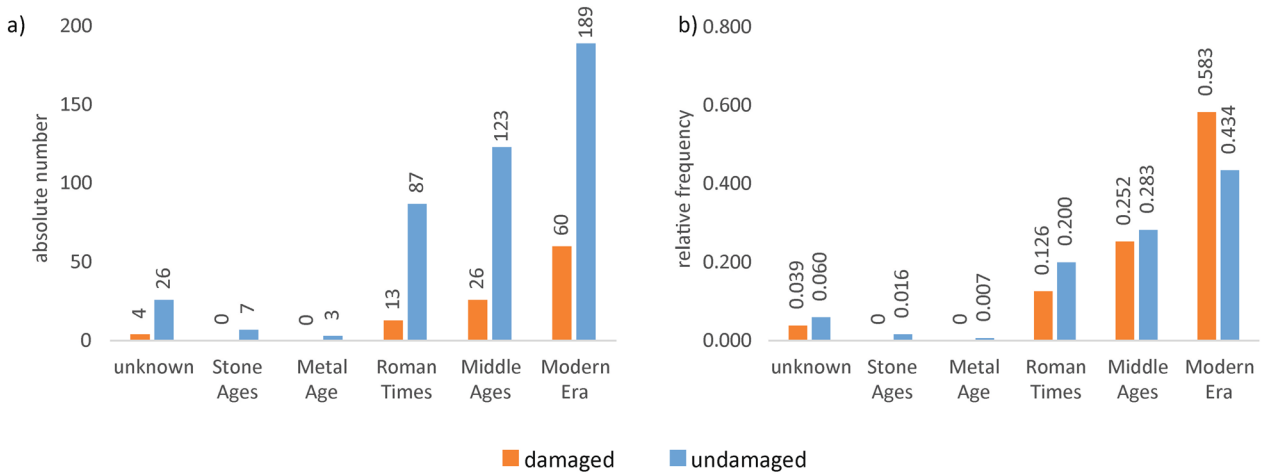


Fig. 5 Absolute (**a**) and relative (**b**) chronological distribution of the surveyed damaged (orange) and undamaged (blue) archaeological sites in the flooded areas. The younger the period, the more sites and the more damage are found

Table 3 Overview of the different types of flood-affected sites

	damaged	*undamaged*	*all*
hydropower (grinding/milling) system	51	157	208
castle / monastery / quadrangle	12	67	79
water management	10	19	29
path / ford / bridge	7	23	30
fall shaft / adit	5	13	18
charcoal kiln / smelting site	5	9	14
war relicts (WWII)	3	28	31
other industrial monuments	3	8	11
villa rustica	2	42	44
ditch / earth bank	-	20	20
city / settlement	-	17	17
grave /burial ground	-	8	8
quarry	-	4	4
others	5	20	25
Sum	103	435	583

caused by alluvial soil, material displacement or landslides. In a few cases, underground cavities collapsed, e.g. an adit or a medieval canal. The temporal correlation of these events with the flood event suggests that they were caused by high levels of soil moisture and/or erosion of underground structures.

In order to better understand the causes of damage, additional characteristics of the damaged sites were also considered: the current use of the area of the archaeological site before the flood (where information was available), the (reconstructed) previous condition of the archaeological site and the material damaged by the flood. In terms of use, almost 20% of the damaged sites are located in a museum/tourist context and are maintained and marked accordingly for the public, e.g. with information boards or railings. A further 30% were in private use or under similar management of the area, most of which were either well maintained or sealed, e.g. by buildings. Sites in a museal/touristic context and in private use are dominated by officially registered monuments. The remaining sites with no apparent use (50%) contain few registered monuments, and were found in most cases of unmaintained or unknown pre-flood condition. In terms of damaged materials, sediments containing cultural layers and masonry/foundation areas were damaged by the flood in almost equal proportions (around 45% each). Constructions made of wood or concrete were seldom encountered, but even here, massive damage, e.g. for the latter by pressure, abrasion or even scouring to relics of the Second World War, such as bunkers or bridges, was sporadically observed.

External factors influencing the effects of the heavy rain and flood event

In addition to the internal factors analysed above, an analysis of internal and external factors is carried out. From an extensive catalogue of different physiographic parameters (Table 2), the Naive Bayes and discriminant analysis methods were used to identify factors that were particularly good at predicting or classifying the occurrence of damage. As the Naïve Bayes approach outperformed the discriminant analysis in all cases, only the results of the former are summarised in Table 4. Note that some variables from Table 2 were excluded before or during the statistical analysis. These were highly correlated parameters and those that did not show a clear causality to the occurrence of damage in archaeological contexts.

Table 4 The results of the statistical assessment of damage dependencies on external factors using Naïve Bayes, including relative and absolute importances (Rank and BIC) as well as accuracy ratings (total, damaged, and undamaged). Results are provided for each river catchment individually and for the combined dataset

Catch-ment	*Statis-tic*	*Site Type*	*Site Chron*	*DLM*	*Erodi-bility*	*Distance to river*	*Slope mean*	*Aspect*	*REM mean*	*Cost dist. mean*	*River flow acc. Max*	*River prec. acc. max*	*Accur. for ‚yes ' ‚*	*Accur. for ‚no ' ‚*	*Overall accur*
Inde	Rank	1	8	2	9	7	10	11	6	3	5	4	77.8	98.4	93.9
	BIC	0.330	0.415	0.344	0.416	0.385	0.443	0.446	0.376	0.345	0.361	0.353			
Rur (Olef Urft)	Rank	10	9	2	11	4	3	1	6	5	7	8	74.1	94.6	89.1
	BIC	0.466	0.443	0.381	0.467	0.384	0.382	0.379	0.411	0.402	0.423	0.437			
Erft	Rank	9	10	5	11	4	7	8	6	1	2	3	40.0	96.3	88.9
	BIC	0.354	0.356	0.308	0.377	0.307	0.328	0.335	0.320	0.295	0.298	0.302			
Wupper	Rank	11	6	1	3	7	4	5	2	10	9	8	39.1	93.6	82.9
	BIC	0.477	0.414	0.390	0.399	0.426	0.405	0.407	0.394	0.456	0.440	0.439			
All	Rank	9	10	5	1	8	11	6	7	3	4	2	39.8	91.7	81.8
	BIC	0.426	0.433	0.410	0.404	0.425	0.447	0.412	0.418	0.407	0.407	0.404			

At first sight, the approach shows high overall accuracies between 80 and 95% in predicting the state of sites after the event. However, these overall accuracies are largely driven by the high percentage of successfully predicted undamaged sites while damaged sites were predicted correctly at much lower rates, down to below 40%. This suggests that there are too few similarities between damaged sites regarding external factors to allow for an accurate prediction based on this multi-factor approach. This is particularly true when combining the sites of all catchments, where the accuracies are generally lowest. In addition, the relative and absolute importance of external factors in predicting the conditions of sites, as indicated by the rank and BIC, respectively, varies greatly between the catchments. This is indicative of the heterogeneity of the catchments and the damage therein. It also means that the approach cannot identify a universally applicable set of external factors for predicting flood-related damage.

The results of the χ^2 approach to the internal and external parameter listed in Table 5 show that only four parameters show statistical independence when comparing damaged and undamaged sites. The results, however, often require the consideration of additional factors (external or internal) and are therefore already discussed here in more detail. The current use of the landscape, represented by a simplified classification of the DLM data (Table 2), revealed an overrepresentation of damage occurring in forested areas and within waterbodies. In contrast, agrarian or built-up landscapes (urban and industrial areas, open mining areas, etc.) showed less damage. A relation between the erodibility of the soil showed that there was more damage on soils with a K-factor between 0.3 and 0.5, significantly more than expected from the overall distribution (Fig. 6:a). Counterintuitively, highly erodible soils (>0.5) showed little damage. The spatial distribution of easily erodible soils, indicated in Fig. 3:a could provide an explanation for this: the distribution indicates that most easily erodible soils (e.g. loessic soils) are located in the lowlands, where the destructive force of the flood was comparatively low due to slower flow velocities (compare Table 1).

The distance of a site from a flowing river does not show a significant pattern of damage. However, the data set is heavily biased towards potentially flooded areas due to the methodological approach used to select the sites. All cases where damage was found outside the flood risk areas refer to reported damage caused exclusively by slope water.

The slope parameter (Fig. 6:b) calculated for the area of each archaeological site showed a correlation between the slope intensity and the occurrence of damage. In general, the relative frequency of damage increases for sites with a slope mean value of 10° and above, the χ^2 test does indicate statistical independence. In addition, the number of medium to high/intensive damage peaks, especially for sites with slopes between 10° and 20°. The overall picture is again, however, slightly distorted by the microtopography of the damaged areas, which occur frequently near (often anthropogenic) bank slopes and river cliffs (cut banks). For the following parameter, the aspect of areas with archaeological sites (measured in 360°), we assumed that human settlement became increasingly independent of factors such as favourable microclimatic conditions in the course of the Middle Ages and especially the modern period. The aspect factor (Fig. 6:c) should therefore play a subordinate role. In fact, although the relative frequency of south-facing slopes is somewhat higher, the results do not indicate a statistical independence of damaged and undamaged sites (Table 5).

For the mean value derived as the relative elevation model (REM, i.e. the elevation of a site above the next river) as well as the cost distance (taken as an indicator for the likeliness that water reached a site), there is no clear trend in expected damage. The last parameter, river flow accumulation (Fig. 6:d) indicates a slight tendency of more damage than expected for sites with an upstream area ranging between 60 and 240 km^2, and with less damage for sites with smaller upstream areas and with larger accumulation values, the latter probably because flow velocity becomes less intense in lowland regions. The problem with interpreting this observation, as with the river precipitation accumulation parameter (Table 2) is that this parameter is influenced by many other factors, such as catchment size, precipitation intensity, slope, etc., so its complexity precludes any prediction based on it alone.

Remote sensing – evaluating ALS elevation data in the context of flood damage

The ALS methodology outlined above was applied as a case study to a large historic mining area ('Grube Glücksthal') located in the Eifel [40]. Here, the terrain surfaces were first interpolated (Fig. 7:a = 2017; Fig. 7:b = 2021) from the two ALS point data sets, and then the difference between these two surfaces was calculated (Fig. 7:c). The 1 m × 1 m grid squares without ALS ground points are coloured dark green (Fig. 7:c). The calculation of contour lines for the difference map allowed delineation of the areas with a possible loss of more than 0.45 m. Disregarding the areas without ground points in any of the two point clouds and very small areas resulted in 25 possible loss areas, nine of which are visible in the map sections in Fig. 7.

Table 5 Results from the χ^2 test performed for several parameter (see Table 4) comparing damaged and undamaged archaeological sites. All parameters showing statistical independence are marked with an *

	χ^2	*p*		*d. f*
Site type	32.713	***0.003***	*	14
Site Chronology	8.8681	0.064		4
DLM	11.208	***0.010***	*	3
Erodibility	12.538	***0.028***	*	5
Distance to river	10.769	0.096		6
Slope mean	38.97	***< 0.001***	*	6
Aspect	5.429	0.710		8
REM mean	6.3993	0.171		4
Cost dist. mean	8.0955	0.151		5
River flow acc. max	8.7979	0.117		5
River prec. acc. max	8.223	0.144		5

During the fieldwork in October 2022, only loss zones numbered 1 and 2 were recorded by the project team. The example of the Grube Glücksthal shows the potential of the method in a large facility that is partly difficult to access and inspect, where the ground is covered by fallen leaves and maintenance is not regularly conducted. The availability of ALS data just a few months after the damage was a prerequisite for a good result.

Another case study dealing with the damage of a weir and a canal clearly demonstrates the approach's limitations [40]. The ALS data recorded in March 2022 show the result of substantial works in the riverbed after the flood. A major drawback is that the ALS data from Geobasis NRW does not record the terrain covered by water, and the ALS points on water are mostly in the ground point class. Therefore, the ALS data comparison did not allow for the identification of damage to the submerged parts of the weir nor for the reliable delineation of the watercourse in the vicinity of the weir before and after the flood event. Photographs taken in the field were needed to distinguish between relocated parts of the weir and a pile of large stones that now protect parts of the weir. In this case, drone-based imagery showing the construction activity shortly after the flood provides the best data on the remains of this site.

The large database of damage documented during the on-site visits made it possible to investigate the potential

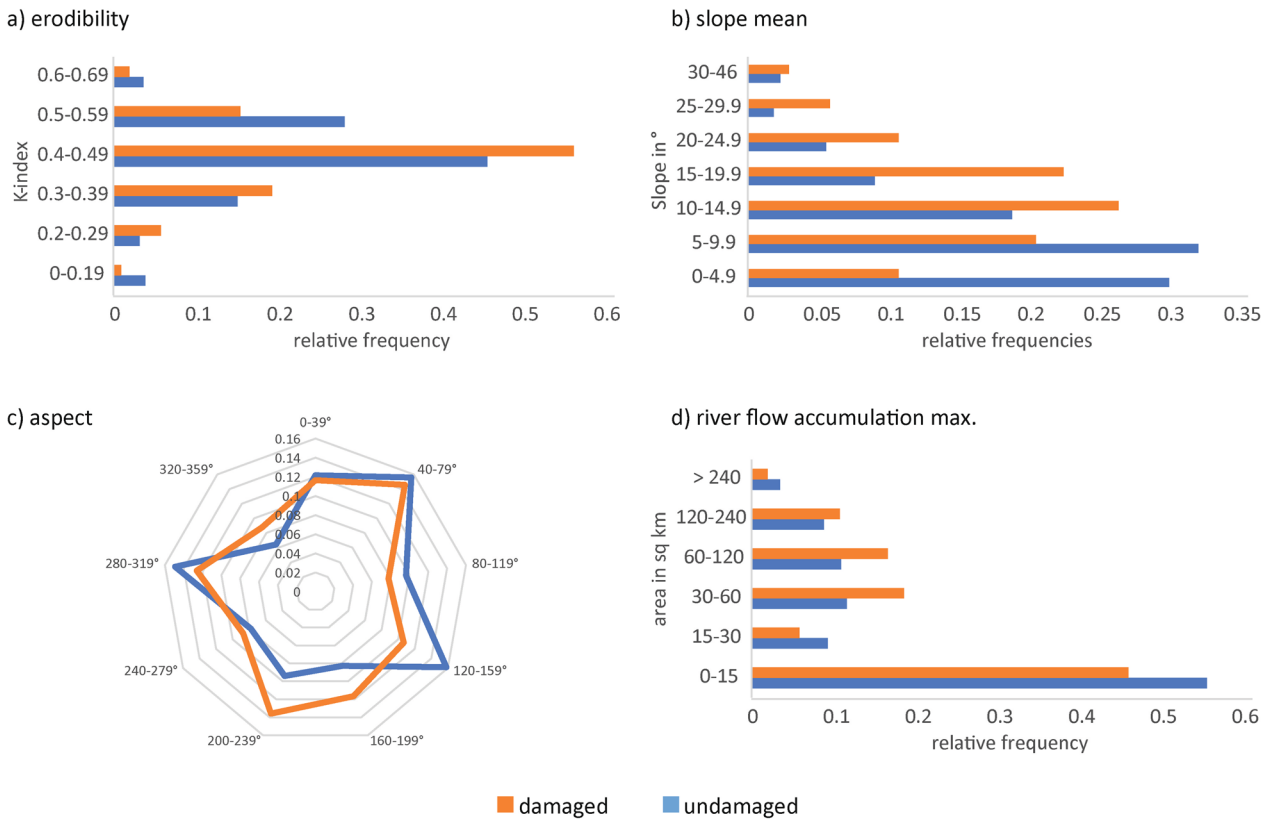


Fig. 6 Relative frequencies of different external parameter for damaged and undamaged sites. **a** erodibility (K-factor); **b** slope mean (given in degree); **c** aspect (given in 360°), and **d** river flow (stream) accumulation (area in km^2), calculated for all sites (n = 539). For details on parameters see Table 2

of ALS data, as provided by Geobasis NRW, for detecting flood-related damage. Our research revealed that this approach could only identify up to 44% of the cases, even if the ALS data were readily available [40]. In most cases (49%), the visibility and recognisability of the damage is clearly impaired. For 7% of the damaged sites, no statement could be made. The impairment depended on several factors. Often, the damaged parts were hidden by walls or other construction remnants of the site (n = 28). As mentioned above, the used ALS data from Geobasis NRW could not identify damage under water. In four cases, the damaged areas of Roman aqueduct remains were concealed by protective structures. In only a few of the remaining cases, the damage was either close to the surface and of an insignificant extent, or it involved displaced components that are generally unsuitable for detection by ALS (n = 7). Finally, and importantly for the evaluation, another 12 cases would not have been detectable in the present sample because the damage was repaired or mitigated immediately after the flood event. This was particularly the case when important infrastructure in the vicinity was affected.

Discussion

The 'Flood Damage Register 2021' allowed us to quantify and characterise the extent and nature of the damage caused by the extreme rain- and flood event. Almost half of the recorded damage required urgent action to protect or preserve the archaeological heritage, while minor damage (17%) was comparatively rare. The damaging effects of the catastrophic event appeared to be stochastic and related to complex situational contexts. Archaeological sites in the affected areas were generally very diverse in terms of protection, preservation, and material. This also affected the potential of using the ALS data approach after this catastrophic event to detect damage. Besides the inherent properties of the sites themselves, which made almost half of the damage not detectable, the delayed availability of post-flood ALS data was problematic too (in the case of the 2021 event, they were not available even after more than two years for large parts of the study area), and also the necessary computing capabilities and required error-checks (e.g. the aligning the elevation data sets in terms of location or height before calculating the difference [40]), impede larger-scale, explorative calculations. However, there is a

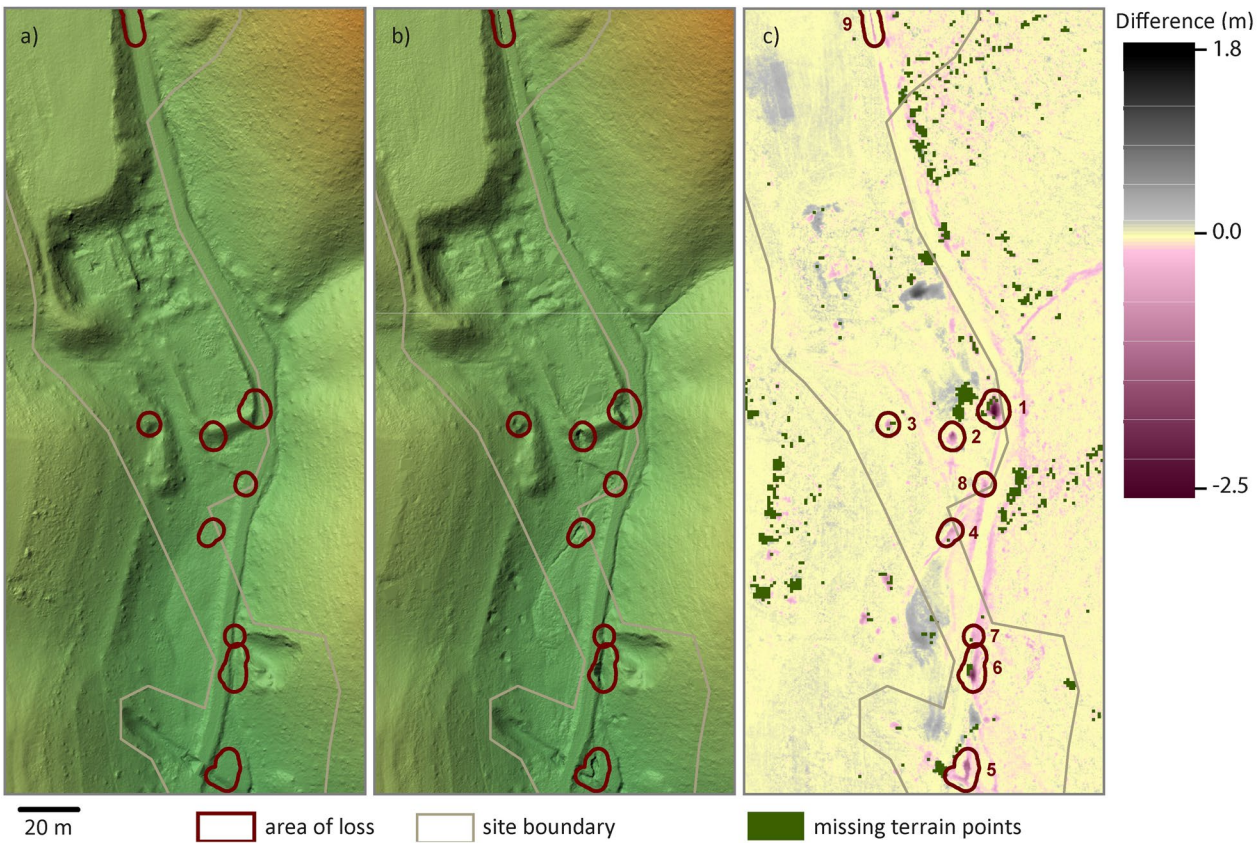


Fig. 7 Part of the southern section of the Grube Glücksthal, mining area (Bad Münstereifel). Terrain model from **a** 2017 compared with **b** December 2021; **c** map of differences

lot of potential in combining drone-based aerial imagery with ALS using different sensors, higher resolution and adapted point classification algorithms to avoid some of the above mentioned drawbacks. For example, it is possible to use ALS sensors that support wavelengths where the laser beam is not reflected on a clear water surface [41]. Tailor-made point classification could also lead to the inclusion of points on walls in the relevant point list for interpolation [41]. An optimal combined aerial and ALS survey of all relevant archaeological sites in the Rhineland serving as a baseline for future monitoring is currently beyond the means of the LVR-ABR. Without dense vegetation, it is possible to document damage using our organisation's drone-based photography and to use ordnance survey ALS data for comparison [42]. However, if only one side of the watercourse is accessible, georeferencing 3D data derived from drone recordings is a problem when relying on ground control points. In the future, drone-based ALS data collected shortly after a disaster may overcome the problem of dense vegetation. For now, our results underline the importance of on-site inspection.

The archaeological database showed that although the flood affected a wide variety of archaeological site types from different periods, damage to modern archaeological sites was significantly more frequent at the scale level of the study area. On the one hand, this finding is biased by factors such as the visibility of sites and (therefore) the detectability of damage. Especially in the lowlands, older settlements are hidden under the sediments of the floodplains [43, 44]. On the other hand, the massive structural development of the river valleys in the study area has influenced the preservation of the archaeological heritage landscape. While this influence has been particularly intense in the last few centuries, the deposition and redeposition of extensive colluvial and alluvial deposits caused by human intervention have been documented for the Lower Rhine Embayment since the Early Bronze Age [45–47]. Historical extreme rainfall and flood events, such as, e.g. between July 19th and 22nd in 1342, repeatedly affected large areas of the low mountain ranges [48, 49]. While the preservation of older archaeological sites in river floodplains is generally considered to be low, a protective and preserving function of precisely the thick soil cover of the colluvium can be observed for certain sites from the Roman period. An example of a negative evidence comes from sites categorised as related to 'water management': most of the damage in this category affected the Roman Eifel Aqueduct [50], a water pipeline more than 100 km long that was particularly damaged in sections where the aqueduct is accessible to tourists, i.e. not covered by soil. More than half of the damaged Roman sites relate to the aqueduct, while the other half includes relics of Roman settlements (*villae rusticae*), the Roman road network, and a Roman smelting site. However, among a total of 44 *villae rusticae* located in the flood risk areas that were assessed, only two were encountered damaged: a very small proportion (5%) compared to the damage within almost all other site types. It is possible that the ancient choice of location itself, as well as the above-mentioned overlying colluvium, are factors for their insensitivity to erosive damage.

While the Erosion of soil material was the most prominent cause of damage to the archaeological sites, it is interesting to note that the deep gully erosion ('*Schluchtenreißen*') already known from hazards from medieval contexts [48, 51], to which slopes in the loess areas of the Rhineland are particularly susceptible, was only rarely observed for the flood event from 2021, at least not outside of already existing erosion gullies. This striking difference may be due to the fieldwork setup, which was largely confined to the streams and flood hazard areas, while the slopes above were generally outside the study area. In the two catastrophic erosion events already mentioned above, i.e. the flooding of the Inden open-cast lignite mine and a gravel pit on the Erft river, the steep, artificially created height differences there favoured retrogressive erosion, which displaced enormous amounts of sediment [5, 25]. From a heritage management perspective, the damage caused to the known archaeological sites in these areas remained relatively minor, but the destruction of unknown sites must be expected.

Our attempt to safely predict the occurrence of damage by applying a multi-factor statistical analysis using Naive Bayes failed to identify a set of external factors that can be used across catchments for this purpose. The main problem was that the accuracy of predicting damage was as low as 40% across the river catchments, indicating a high heterogeneity of external factors within all catchments. This can be interpreted as a high factor of randomness in the spatial distribution of damage events or as a lack of external factors that accurately represent the damage potential. In order to reduce the spatial heterogeneity of damaged sites, it would be advisable to divide the sites into different subsets. These subsets could be based on three different categories: (i) The type of archaeological site. This would be valuable for reducing the variability caused by site-type specific microenvironmental settings and affected materials, such as for water powered milling systems. (ii) The cause of damage. In our case, it was possible to identify outliers within the external factors that were not damaged by river flooding, but by slope-driven erosional processes. (iii) The regional setting. As could be shown in this study, the regional topography plays an important role in influencing both the type of damage

and the overall damage potential of sites. While subsetting was not advisable in this study due to the small sample size of damaged sites, it is very promising for larger studies to potentially reduce the heterogeneity of external factors.

For the external factors in this study, we had access to geospatial datasets describing soil properties, land use, topography and certain hydrological factors. While this large database provides extensive information on site characteristics, the question is whether it can accurately represent the damage potential of a river flood event. This is a particularly complex issue to represent, as the erosional capacity of streams is not determined by local topography but also by upstream properties, causing, e.g. funnelling effects or local turbulence. These complex hydraulic processes can vary greatly over small distances and can only be adequately described by hydraulic models based on complex 3D-models of the riverbed and its surroundings. However, these models require huge amounts of computation power and time to calculate. In addition, accurate 3D-models have yet to be available for most regions. Recent advances in hydraulic modelling highlight promising avenues for the availability and accuracy of such models [52]. Therefore, we see one of the main future potentials for similar multi-factor statistical analyses of flood damage potential to archaeological heritage in implementing hydraulic models as external factors.

Conclusions

The flood affected many areas of the study region with diverse, extensive and intensive cultural landscapes. 19% of the surveyed archaeological sites showed damage that was definitely or very probably caused by the flood. A GIS-based workflow was developed and adapted to identify potentially damaged archaeological sites in the flood hazard area. This allowed a systematic and uniform recording of flood damage to archaeological sites, thus forming a reliable basis for damage mitigation.

From the empirical observations it became clear that damage often could have been anticipated in retrospect. In many cases, however, preventive measures would have been very costly and/or would have obscured the visibility of the archaeological sites. Above-ground visibility and accessibility of the archaeological sites often increased the risk of damage, as has been shown for the Roman Eifel aqueduct. Similarly, constructions such as protective roofs, walls or pavements were not always beneficial for the site during the flood event, as they channelled water and increased its pressure and erosive power. The spatially extensive relics of industrialisation in connection with hydropower, which were frequently affected by flooding, represent a special case. They have so far received little attention with regard to local protection. Cooperation between the numerous responsible authorities involved is necessary to reconcile legal mandates, public and private interests, as well as protection and conservation measures to this element of the cultural landscape.

The comparison of ordnance survey ALS elevation data recorded before and after the flood event is only useful where recent ALS data are available. When focusing on large, land-based sites and sites not protected by a roof, the approach could serve as an assessment tool for areas of interest in a possible planning phase of a similar project. Advantages of this approach include improved damage detection for inaccessible sites, sites with secluded or remote areas, or sites hidden under on-ground cover. Fieldwork, however, is still required to verify the results and to check small or partially submerged sites.

Given the apparent changes in global climate and regional weather regimes, the difficulty in identifying clear external predictors of damage to archaeological sites from hydrometeorological hazards highlights the need to individually consider the specific (micro) location of an archaeological site in relation to potentially extreme flow and slope water. The implementation and improvement of modelling of complex hydraulic processes (see above) and larger-scale extreme flood events [13] are good starting points. Specific parameters relevant to a region, e.g. calamity areas [53] or surface sealing [5], groundwater subsidence or drought, increased wind activity, earthquakes or subsidence could also be considered when determining potential damage from hazards. The detailed data of the database can be further used, e.g. for posterior risk analyses and models predicting future disaster impacts [11, 54]. These applications would also be valuable in identifying risks and long-term consequences in the event of landscape changes.

With priority given to the protection of human life and infrastructure, a new discourse on protecting low mountain regions against extreme flash floods has been launched after the flood event of 2021 [55]. The archaeological heritage has benefitted and will benefit from these larger-scale measurements. However, the specific needs of archaeological sites have to be taken into account when discussing the challenges of climate change for cultural heritage.

Abbreviations

ALS	Airborne Laser Scanning elevation data
LVR-ABR	LVR-State Service for Archaeological Heritage (in the Rhineland)
POI	Point of Interest (intersections of archaeological sites and flood-prone areas)

Acknowledgements

The authors would like to thank Maximilian Formen for his help in creating the maps of Fig. 1, 3, and 4 and the anonymous reviewers for comments that helped to improve the paper. IS, CK, HW would like to thank the staff of the

'LVR-ABR Außenstelle Nideggen-Wollersheim' for their great hospitality and support during the project's fieldwork and writing up of the reports.

Author contributions
IS, BB and IH conceptualised and wrote the paper, BB conducted the geostatistical analysis. CK, HW and IS conducted the fieldwork, compiled and analysed the archaeological database; HW, CK, FL and FS contributed specific aspects to the manuscript and improved its content. All authors read and approved the final version of the manuscript.

Funding
Open Access funding enabled and organized by Projekt DEAL. The 'Flood Damage Register 2021' project was initiated, designed and carried out by the LVR-State Service for Archaeological Heritage. Financial support was provided by the Ministry of Regional Identity, Local Government, Building and Digitalization of the State of North Rhine-Westphalia. The latter had no role in the data analysis and interpretation or in the manuscript's writing.

Availability of data and materials
The data supporting the findings of this study are available from the LVR—State Service for Archaeological Heritage (LVR—Amt für Bodendenkmalpflege im Rheinland) but restrictions apply to the availability of these data, which were used under license for the current study, and are therefore not publicly available. Data are, however, available from the authors upon reasonable request and with permission of LVR—State Service for Archaeological Heritage.

Declarations

Ethics approval and consent to participate
Not applicable.

Consent for publication
Not applicable.

Competing interests
The authors declare no competing interests.

Author details
[1]LVR-State Service for Archaeological Heritage, Endenicher Str. 133, 53115 Bonn, Germany. [2]Present Address: Institute for Prehistoric Archaeology, University of Cologne, Bernhard-Feilchenfeld-Str. 11, 50969 Cologne, Germany. [3]Chair of Physical Geography and Geoecology, Department of Geography, RWTH Aachen University, Wüllnerstr. 5B, 52056 Aachen, Germany. [4]Institute for Prehistoric Archaeology, University of Cologne, Bernhard-Feilchenfeld-Str. 11, 50969 Cologne, Germany.

Received: 11 June 2024 Accepted: 11 September 2024
Published online: 18 September 2024

References

1. Tradowsky JS, Philip SY, Kreienkamp F et al (2023) Attribution of the heavy rainfall events leading to severe flooding in Western Europe during July 2021. Clim Change 176:90. https://doi.org/10.1007/s10584-023-03502-7
2. Junghänel T, Bissolli P, Daßler J, et al (2021) Hydro-klimatologische Einordnung der Stark- und Dauerniederschläge in Teilen Deutschlands im Zusammenhang mit dem Tiefdruckgebiet „Bernd" vom 12. bis 19. Juli 2021. Deutscher Wetterdienst, Geschäftsbereich Klima und Umwelt, Offenbach
3. Mohr S, Ehret U, Kunz M et al (2023) A multi-disciplinary analysis of the exceptional flood event of July 2021 in central Europe – Part 1: Event description and analysis. Nat Hazards Earth Syst Sci 23:525–551. https://doi.org/10.5194/nhess-23-525-2023
4. Blöschl G, Hall J, Viglione A et al (2019) Changing climate both increases and decreases European river floods. Nature 573:108–111. https://doi.org/10.1038/s41586-019-1495-6
5. Lehmkuhl F, Schüttrumpf H, Schwarzbauer J, et al (2022) Assessment of the 2021 summer flood in Central Europe. Environ Sci Eur 34:107, s12302–022–00685–1. https://doi.org/10.1186/s12302-022-00685-1
6. Lehmann J, Coumou D, Frieler K (2015) Increased record-breaking precipitation events under global warming. Clim Change 132:501–515. https://doi.org/10.1007/s10584-015-1434-y
7. Kotova L, Leissner J, Winkler M et al (2023) Making use of climate information for sustainable preservation of cultural heritage: applications to the KERES project. Herit Sci 11:1–18. https://doi.org/10.1186/s40494-022-00853-9
8. Leissner J, Fuhrmann C (2018) Cultural heritage and climate change: are we at the tipping point? Cartadaitalia 1:220–235
9. Sabbioni C, Brimblecombe P, Cassar M (2010) The atlas of climate change impact on European cultural heritage. Anthem Press, New York, Scientific Analysis and Management Strategies
10. Sesana E, Gagnon A, Bertolin C, Hughes J (2018) Adapting cultural heritage to climate change risks: perspectives of cultural heritage experts in Europe. Geosciences 8:305. https://doi.org/10.3390/geosciences8080305
11. Cacciotti R, Sardella A, Drdácký M, Bonazza A (2024) A methodology for vulnerability assessment of cultural heritage in extreme climate changes. Int J Disaster Risk Sci 15:404–420. https://doi.org/10.1007/s13753-024-00564-8
12. ICCROM, ICOMOS, IUCN, UNESCO World Heritage Centre (2014) Managing disaster risks for world heritage: a tool for identifying, assessing and reducing risks for heritage. World Herit Rev 74:47–49
13. Ludwig P, Ehmele F, Franca MJ, et al (2022) A multi-disciplinary analysis of the exceptional flood event of July 2021 in central Europe. Part 2: Historical context and relation to climate change
14. Jigyasu R, King J, Wijesuriya G (2010) Managing disaster risks for world heritage. United Nations Educational, Scientific and Cultural Organization, Paris
15. DSchG NRW (2022) Geltende Gesetze und Verordnungen. Nordrhein-westfälisches Denkmalschutzgesetz (DSchG NRW). In: RECHT.NRW.DE. https://recht.nrw.de/lmi/owa/br_bes_text?anw_nr=2&bes_id=48749&aufgehoben=N&keyword=denkmalschutz. Accessed 4 Dec 2023
16. Koppmann C, Riemenscheider D, Schmidt I et al (2023) Die Flut in Nordrhein-Westfalen und ihre Folgen. Archäol Dtschl 24:48–51
17. Sonntag S, Riemenschneider D, Zeiler M (2022) Michael M (2023) Nach der Jahrhunderflut – Denkmalschäden im Sauerland und südlichen Ruhrgebiet. Archäol Westfal-Lippe 14:259–262
18. Koppmann C, Schmidt I, Witte H (2023) Erste Ergebnisse des Projektes „Schadenskataster Hochwasser 2021". In: Claßen E, Trier M (eds) Archäologie im Rheinland 2022. Nünnerich-Asmus, Oppenheim, pp 23–24
19. Schmidt I, Witte H, Koppmann C (2024) Nach der Flut: Die Auswirkungen des Hochwassers im Juli 2021 auf die Bodendenkmäler im Rheinland. In: Claßen E, Trier M (eds) Archäologie im Rheinland 2023. Nünnerich-Asmus, Oppenheim, pp 24–26
20. Schmidt I, Witte H, Koppmann C (2024) Von der Flut betroffen – ein Schadenskataster archäologischer Fundstellen des Rheinlandes. Archäol Beitr Aus Dem Rheinl 1:1–32
21. Dietze M, Bell R, Ozturk U et al (2022) More than heavy rain turning into fast-flowing water – a landscape perspective on the 2021 Eifel floods. Nat Hazards Earth Syst Sci 22:1845–1856. https://doi.org/10.5194/nhess-22-1845-2022
22. Landesamt für Natur, Umwelt und Verbraucherschutz Nordrhein-Westfalen (LANUV) (2021) Berichte zur hydrologischen Situation in Nordrhein-Westfalen. Übersicht zu den Hydrologischen Lageberichten während des Hochwassers im Juli 2021. In: LANUV Kompet. Für Ein Leb. Land. https://www.lanuv.nrw.de/umwelt/wasser/hydrologische-berichte. Accessed 11 Dec 2023
23. Ministerium für Umwelt, Landwirtschaft, Natur- und Verbraucherschutz des Landes Nordrhein-Westfalen (MULNV) (2021) Sitzung des Ausschusses für Umwelt, Landwirtschaft, Natur- und Verbraucherschutz des Landtags Nordrhein-Westfalen am 9. August 2021, Schriftlicher Bericht Hochwasserereignissen Mitte Juli 2021. 66. Sitzung, Vorlage 17/5485. Ausschuss für Umwelt, Landwirtschaft, Natur- und Verbraucherschutz, Düsseldorf
24. DWD (2024) Hourly precipitation data for Germany based on radar data – RADOLAN. Available via https://opendata.dwd.de/climate_environment/CDC/grids_germany/hourly/radolan/. Accessed 04 Dec 2023.

25. Lehmkuhl F, Weber A, Esser V et al (2022) Fluviale Morphodynamik und Sedimentkontamination bei Extremereignissen: Das Juli-Hochwasser 2021 im Inde-Einzugsgebiet (Nordrhein-Westfalen). Korresp Wasserwirtsch 7:422–427
26. Herzog I, Dortangs R, Weber C (2015) Einsatz einer neuen webbasierten Datenbank mit GIS-Funktionalitäten im LVR-Amt für Bodendenkmalpflege. In: Archäologie im Rheinland 2014. Nünnerich-Asmus, Oppenheim, pp 35–39
27. Landesbetrieb Information und Technik Nordrhein-Westfalen (IT.NRW) (2023) OpenGeodata.NRW. In: Inf. Tech. Nordrh.-Westfal. https://www.opengeodata.nrw.de/produkte/. Accessed 4 Dec 2023
28. Kisseler E (2022) Land use in the context of extreme flood events – how should we plan for the future?
29. CEMS (2021) Copernicus Emergency Management Service. Available via https://emergency.copernicus.eu. Accessed 04 Jan 2023.
30. EFAS (2021) Copernicus, European Flood Awareness System. Available via https://www.efas.eu/en. Accessed 04 Dec 2023.
31. Lindsay JB, Cockburn JMH, Russell HAJ (2015) An integral image approach to performing multi-scale topographic position analysis. Geomorphology 245:51–61. https://doi.org/10.1016/j.geomorph.2015.05.025
32. Kovarovic K, Aiello LC, Cardini A, Lockwood CA (2011) Discriminant function analyses in archaeology: are classification rates too good to be true? J Archaeol Sci 38:3006–3018. https://doi.org/10.1016/j.jas.2011.06.028
33. Davis J, Sampson R (1986) Statistics and data analysis in geology. Wiley, New York
34. Armero C, Garcıa-Donato G, Jiménez-Puerto G, et al A Bayesian naıve Bayes classifier for dating archaeological sites. In: Proceedings of the 35 th International Workshop on Statistical Modelling IWSM 2020. Universidad del País Vasco
35. Monna F, Magail J, Rolland T et al (2020) Machine learning for rapid mapping of archaeological structures made of dry stones – Example of burial monuments from the Khirgisuur culture, Mongolia –. J Cult Herit 43:118–128. https://doi.org/10.1016/j.culher.2020.01.002
36. Hesse R (2016) Possibilities and challenges in the application of multitemporal airborne lidar data sets for the monitoring of archaeological landscapes. In: Börner W, Uhlirz S (eds) Proceedings of the 20th International Conference on Cultural Heritage and New Technologies 2015. Wien, Österreich, pp 1–9
37. Wheatley D, Gillings M (2002) Spatial technology and archaeology: the archaeological applications of GIS, 1. publ. Taylor & Francis, London
38. Herzog I (2021) Vom Niedergang einer Landwehr. In: Claßen E, Trier M (eds) Archäologie im Rheinland 2020. Nünnerich-Asmus, Oppenheim, pp 36–39
39. Beex W (2004) Use and Abuse of Digital Terrain/Elevation Models. In: Stadtarchäologie Wien (ed) Enter the past: the E-way into the four dimensions of cultural heritage: CAA 2003, Computer Applications and Quantitative Methods in Archaeology: proceedings of the 31st conference, Vienna, Austria, April 2003. Archaeopress, Oxford, England, pp 240–242
40. Herzog I, Schmidt I, Koppmann C (2024) Nach dem Hochwasser – Schadensdokumentation am Computer? In: Claßen E, Trier M (eds) Archäologie im Rheinland 2023. Nünnerich-Asmus, Oppenheim, pp 27–30
41. Doneus M, Mandlburger G, Doneus N (2020) Archaeological Ground Point Filtering of Airborne Laser Scan Derived Point-Clouds in a Difficult Mediterranean Environment. J Comput Appl Archaeol 3:92–108. https://doi.org/10.5334/jcaa.44
42. Cott E, Dujmovič T, Klinke L, et al (2023) Vermessung des Schadens – Bodendenkmäler und Waldsterben. In: Claßen E, Trier M (eds) Archäologie im Rheinland 2022. Nünnerich-Asmus, Oppenheim, pp 25–28
43. Schmidt-Wygasch C (2010) Neue Untersuchungen zur holozänen Genese des Unterlaufs der Inde: chronostratigraphische Differenzierung der Auelehme unter besonderer Berücksichtigung der Montangeschichte der Voreifel. Fakultät Georessourcen und Materialtechnik. Geographisches Institut, Rheinisch Westfälische Technische Hochschule Aachen
44. Schmidt-Wygasch C, Schamuhn S, Meurers-Balke J, et al (2010) Indirect dating of historical land use through mining: Linking heavy metal analyses of fluvial deposits to archaeobotanical data and written accounts. Geoarchaeology 25:837–856. https://doi.org/10.1002/gea.20334
45. Lehmkuhl F, Schulte P, Römer W, Pötter S (2023) The loess landscapes of the Lower Rhine Embayment as (geo-)archeological archives – insights and challenges from a geomorphological and sedimentological perspective. EG Quat Sci J 72:203–218. https://doi.org/10.5194/egqsj-72-203-2023
46. Protze J (2014) Eine "Mensch-gemachte Landschaft": Diachrone, geochemische und sedimentologische Untersuchungen an anthropogen beeinflussten Sedimenten und Böden der Niederrheinischen Lössbörde. Dissertation, RWTH Aachen University
47. Schulz W (2006) Die Kolluvien der westlichen Kölner Bucht. Universität zu Köln, Gliederung, Entstehungszeit und geomorphologische Bedeutung
48. Brand C, Gerlach R, Meurers-Balke J (2008) Die Frühgeschichte den Hang hinunter: Schluchtenreißen in Muffendorf. In: Archäologie im Rheinland 2007. Nünnerich-Asmus, Oppenheim, pp 132–135
49. Herget J, Kapala A, Krell M et al (2015) The millennium flood of July 1342 revisited. CATENA 130:82–94. https://doi.org/10.1016/j.catena.2014.12.010
50. Grewe K, Brinker W (1986) Atlas der römischen Wasserleitungen nach Köln. Rheinland-Verlag, Köln
51. Bork H-R (1998) Landschaftsentwicklung in Mitteleuropa: Wirkungen des Menschen auf Landschaften, 1st ed. Klett-Perthes, Gotha
52. Kumar V, Sharma K, Caloiero T et al (2023) Comprehensive Overview of Flood Modeling Approaches: A Review of Recent Advances. Hydrology 10:141. https://doi.org/10.3390/hydrology10070141
53. Cott E (2023) Klimainduzierter Waldumbau und Bodendenkmäler im Wald. In: Kulturerbe im Wald schützen und nutzen: Dokumentation des Fachforums "Kulturerbe in Wäldern gemeinsam erkennen und schützen" am 8. und 9. September in Königswinter und Eitorf (Nordrhein-Westfalen). Bund Heimat und Umwelt in Deutschland (BHU), Bonn, pp 37–44
54. Ehmele F, Kautz L-A, Feldmann H et al (2022) Adaptation and application of the large LAERTES-EU regional climate model ensemble for modeling hydrological extremes: a pilot study for the Rhine basin. Nat Hazards Earth Syst Sci 22:677–692. https://doi.org/10.5194/nhess-22-677-2022
55. Schüttrumpf H, Birkmann J, Brüll C et al (2022) Herausforderungen an den Wiederaufbau nach dem Katastrophenhochwasser 2021 in der Eifel. Dresdner Wasserbauliche Mitteilungen 68:5–16

Publisher's Note

Springer Nature remains neutral with regard to jurisdictional claims in published maps and institutional affiliations.